Insertion, Conductivity, and Structures of Conjugated Organic Oligomers in Self-Assembled Alkanethiol Monolayers on Au{111}

M. T. Cygan,[†] T. D. Dunbar,[†] J. J. Arnold,[†] L. A. Bumm,[†] N. F. Shedlock,[†] T. P. Burgin,[§] L. Jones II,[§] D. L. Allara,*[,‡] J. M. Tour,*[,§] and P. S. Weiss*[,†]

Contribution from the Departments of Chemistry and Materials Science and Engineering, The Pennsylvania State University, University Park, Pennsylvania 16802-6300, and Department of Chemistry and Biochemistry, University of South Carolina, Columbia, South Carolina 29208

Received October 2, 1997. Revised Manuscript Received December 8, 1997

Abstract: Alkanethiolate self-assembled monolayers on Au{111} are used for the two-dimensional matrix isolation of conjugated organic thiolates, studied for their potential to act as molecular wires. The conjugated organic molecules are inserted from dilute solution into boundaries between structural domains and at substrate step edges of preassembled *n*-alkanethiolate monolayers so as to preserve the order of the initial alkanethiolate lattice. In contrast, when both molecules are codeposited from a single solution, the structure of the assembled monolayer shows no ordered molecular lattice of the alkanethiol component. Scanning tunneling microscopy measurements on the isolated conjugated component molecules show them to have enhanced conductivity compared to neighboring alkanethiolates.

I. Introduction

Functionalized organic monolayers are of substantial current interest because of their ability to modify the chemical and physical properties of the substrate surfaces to which they are bound and to provide a variety of chemically tailored surfaces.[1] Recently, great progress has been made in using these monolayers to create surface chemical patterns using micron-scale mask[2] or microcontact printing[3] techniques. Such complex surfaces have been proposed for applications to molecule-specific sensors and nanometer-scale electronics.[4] However, to provide such surfaces, a greater understanding of the structure and stability of multicomponent monolayers on the nanometer scale is needed. One critical aspect of this problem is controlling the state of mixing of adsorbate molecules which differ greatly in one or more structural elements—e.g., terminal functional group, molecular length, and chain substitution. In monolayers containing alkanethiolate molecules, previous studies have found that films can be constructed in which one component will distribute randomly in a matrix of a second component,[5,6] segregate into domains,[7] or be displaced from the film into solution by the second component.[8] These various processes are highly condition-dependent, enough so that we anticipate being able to use them to control the structures of mixed composition films.

A major issue in these spatially controlled multiple component monolayers is characterization at the molecular scale. While macroscopic analytical methods such as wetting, ellipsometry, infrared spectroscopy, and X-ray photoelectron spectroscopy have been successfully used to characterize the *average* film compositions of mixed systems, real-space techniques such as scanning probe microscopies offer a molecular-scale view of the surface structure. Recent scanning tunneling microscope (STM) investigations have yielded molecular resolution images of both single composition and mixed composition self-assembled monolayers (SAMs).[6,9,10] In these images, the positions of individual molecules in the film are determined, and individual molecules have been differentiated. This is an initial step toward imaging a surface and determining which sites exhibit the correct geometry and chemistry for recognition of a specific molecule.

We have been constructing complex surfaces with electronically interesting molecules with the long-range goal of testing the feasibility of molecular electronic devices.[10] In a preliminary report, we showed that these molecules can be imbedded in self-assembled *n*-alkanethiolate films, chosen for their crystallinity and insulating nature. These SAMs chemically and electrochemically isolate the underlying substrates from their surroundings.[11−13] The molecules of interest are then diluted and isolated by the alkanethiolate SAM matrix. This allows

* To whom correspondence should be addressed.
[†] Department of Chemistry, The Pennsylvania State University.
[‡] Departments of Chemistry and Materials Science and Engineering, The Pennsylvania State University.
[§] University of South Carolina.

(1) For example, (a) Ulman, A. *An Introduction to Ultrathin Organic Surface Films*; Academic: San Diego, 1991. (b) Waldeck, D. H.; Beratan, D. N. *Science* **1993**, *261*, 576−577, and references therein.
(2) Rozsnyai, L. F.; Wrighton, M. S. *Langmuir* **1995**, *11*, 3913−3920.
(3) Kumar, A.; Abbott, N. L.; Kim, E.; Biebuyck, H. A.; Whitesides, G. M. *Acc. Chem. Res* **1995**, *28*, 219−226.
(4) Allara, D. L. *Biosensors and Bioelectronics* **1995**, *10*, 771−783. Datta, S.; Tian, W.; Hong, S.; Reifenberger, R.; Henderson, J. I.; Kubiak, C. P. *Phys. Rev. Lett.* **1997**, *79*, 2530−2533.
(5) Takami, T.; Delamarche, E.; Michel, B.; Gerber, Ch.; Wolf, H.; Ringsdorf, H. *Langmuir* **1995**, *11*, 3876−3881.
(6) Bumm, L. A.; Arnold, J. J.; Dunbar, T. D.; Allara, D. L.; Weiss, P. S. Submitted for preparation.
(7) (a) Stranick, S. J.; Parikh, A. N.; Tao, Y.-T.; Allara, D. L.; Weiss, P. S. *J. Phys. Chem.* **1994**, *98*, 7636−7646. (b) Atre, S. V.; Liedberg, B.; Allara, D. L. *Langmuir* **1995**, *11*, 3882−3893.
(8) Folkers, J. P.; Laibinis, P. E.; Whitesides, G. M.; Deutch, J. *J. Phys. Chem.* **1994**, *98*, 563−571.
(9) Camillone III, N.; Eisenberger, P.; Leung, T. Y. B.; Scoles, G.; Poirier, G. E.; Tarlov, M. J. *J. Chem. Phys.* **1994**, *101*, 11031−11036. Delamarche, E.; Michel, B.; Gerber, Ch.; Anselmetti, D.; Guntherodt, H.-J.; Wolf, H.; Ringsdorf, H. *Langmuir* **1994**, *10*, 2869−2871.
(10) Bumm, L. A.; Arnold, J. J.; Cygan; M. T.; Dunbar, T. D.; Burgin, T. P.; Jones II, L.; Allara, D. L.; Tour, J. M.; Weiss, P. S. *Science* **1996**, *271*, 1705−1707.

S0002-7863(97)03448-3 CCC: $15.00
Published on Web 03/13/1998

us to probe the properties of the molecules isolated from each other in the SAM using the STM. In particular, interest in the creation of nanometer-scale electronic devices has led us to develop methods for creating isolated sites of high conductivity within an insulating film. We have developed a rational and simple approach to this problem. Here we expand on our preliminary report which showed the insertion of a highly conjugated molecule, 4-(2′-ethyl-4′-(phenylethynyl)phenylethynyl)-1-phenylthiolate (**1**), into a nominally complete alkanethiolate matrix.[10] When bound to the Au{111} surface, the thiol (**1a**) deprotonates to become the thiolate **1**. This molecule is representative of a family of linear conjugated oligomers having a phenylene ethynylene backbone which have been proposed as candidates for application as "molecular wires".[14] We find that **1**, and similar structures, can be inserted into nominally complete alkanethiolate self-assembled monolayers at film defects, e.g., structural domain boundaries and substrate step edges, such that the insertion process does not disturb the overall translational ordering of the *n*-alkanethiolate lattice. We observe the inserted molecules to be anchored at substrate step edges and at the boundaries between ordered alkanethiolate structural domains. In contrast, in films formed by coadsorption of alkanethiol and **1a** molecules, even at low (10% of **1a**, 90% alkanethiol) solution compositions, the presence of **1** disturbs the overall molecular ordering to such an extent that no alkanethiolate lattice is observed in STM images. Note that Dhirani et al. found that a molecule related to **1**, but lacking the ethyl substituent, can form an ordered monolayer of pure composition on Au{111}.[15] Our methods of isolating linear conjugated molecules in alkanethiolate matrixes have allowed us to make measurements of the electronic properties of isolated molecules. Through these measurements we find evidence for enhanced conductivity of these conjugated molecules as compared to the surrounding alkanethiolate.[10]

II. Experimental Section

II.A. Synthesis. Chart 1 displays the chemical structures of the molecules studied. The preparations are described elsewhere[14] except as noted below. Although the thiol derivative (**1a**) is desired for SAM formation, it is susceptible to air oxidation.[14b] Therefore, the more stable thioacetate derivative (**1b**) was synthesized. The thiol could then be generated in situ during SAM formation by hydrolysis with an addition of base (6 μL of 30% NH_4OH per mg of **1b**).[14b] The molecules **2a** and **3a** were prepared in a similar fashion from **2b** and **3b**, respectively. When bound to the Au{111} surface, we expect them to be in the thiolate forms, **2** and **3**, respectively.

General. The details of the solvent treatment, chemical suppliers, and coupling procedures have been described previously.[14a,c]

Compound 2b (4′-Thioacetylphenyl)ethynyl-4-nitrobenzene (2b). Used were 4-(thioacetylphenyl)ethyne[14c] (0.25 g, 1.4 mmol), 4-iodonitrobenzene (0.28 g. 1.13 mmol), bis(triphenylphosphine)palladium-(II) chloride (40 mg, 0.057 mmol), copper(I) iodide (22 mg, 0.12 mmol), triphenylphosphine (61 mg, 0.23 mmol), *N*,*N*′-diisopropylethylamine (1 mL, 5.5 mmol), THF (2 mL), and powdered 4 Å molecular sieves

Chart 1

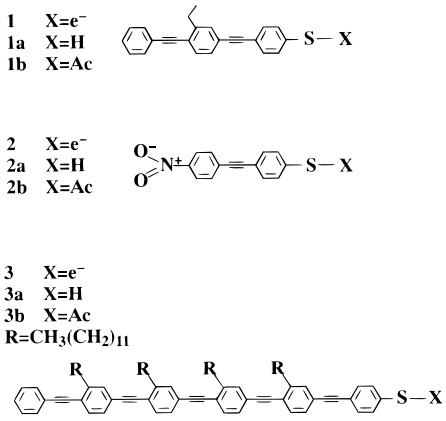

(∼0.5 g) at room temperature for 2 days. The reaction solution was diluted with dichloromethane and extracted with pH 7.0 phosphate buffer. The organic layer was dried with sodium sulfate and evaporated to an orange oil. The crude material was dissolved in a minimal amount of dichloromethane and eluted through a 4.5 16 cm column of silica gel (treated with 2% v/v of bis(trimethylsilyl)acetamide) using 1:2 dichloromethane:hexanes as the eluent. The product was obtained as a yellow powder (0.22 g, 28%) and was extremely prone to deacylation under basic conditions. See Supporting Information for spectroscopic feature details.

Compound 3b (see Chart for Structure). Iodobenzene (0.067 g, 0.60 mmol) was coupled with the thioacetyl-containing pentamer (compound **81** in ref 14a) (0.19 g, 0.15 mmol) in THF (2 mL) using bis(dibenzylideneacetone)palladium(0) (0.017 g, 0.030 mmol), triphenylphosphine (0.020 g, 0.075 mmol), copper(I) iodide (0.0057 g, 0.030 mmol), *N*,*N*′-diisopropylethylamine (0.42 mL, 2.40 mmol) for 2 days to afford 0.13 g (65%) of the title compound as a waxy yellow solid after gravity liquid chromatography (24:1; hexane:ethyl acetate). See Supporting Information for spectroscopic feature details.

II.B. Sample Preparation. Two types of substrates were used in these studies: epitaxial Au on mica (Au/mica) for STM and Au deposited on a thin Cr adhesion layer on a surface-oxidized Si wafer (Au/Cr/SiO_2/Si) for reflection absorption infrared spectroscopy (IRS), ellipsometry, and other studies.[16] Substrates for STM studies were prepared by resistive evaporation of gold (99.999%) onto the surface of freshly cleaved mica which was preheated in a vacuum to 380 °C. The base pressure in the chamber during evaporation was maintained $\leq 2 \times 10^{-7}$ Torr. After 120 nm of gold was deposited at 0.1 nm/s, the substrate temperature was returned to <30 °C while still under vacuum. Then the chamber was back-filled with purified nitrogen, the substrates transferred into an inert atmosphere and immersed immediately in the thiol solutions (described below). Companion substrates for IRS and other studies were prepared by evaporating 10 nm of chromium as an adhesion layer, followed by 200 nm gold onto cleaned surfaces of polished, native oxide-covered single crystal Si(100) wafers according to a previously reported procedure.[16,17] The silicon wafer surfaces were precleaned by immersing the samples in a 1:4 mixture of H_2O_2/H_2SO_4 at 110 °C for 10−15 min (*Warning: this solution reacts strongly with organic compounds and should not be stored in closed containers. It must be handled with extreme caution.*), followed by rinses in deionized purified water[18] and absolute ethanol. The freshly prepared Au/Cr/SiO_2/Si samples were immediately characterized using single wavelength ellipsometry and then immersed directly (maximum ambient exposure of 5 min) into the thiol solutions.

(11) Haran, A.; Waldeck, D.; Naaman, R.; Moons, E.; Cahen, D. *Science* **1994**, *263*, 948−950. Chidsey, C. E. D. *Science* **1991**, *251*, 919−922. Rubin, S.; Chow, J. T.; Ferraris, J. P.; Zawodzinski, T. A., Jr. *Langmuir* **1996**, *12*, 363−370.

(12) Chailapakul, O.; Sun, L.; Xu, C.; Crooks, R. M. *J. Am. Chem. Soc.* **1993**, *115*, 12459−12467.

(13) Takehara, K.; Takemura, H.; Ide, Y. *J. Coll. Interfac. Sci.* **1993**, *156*, 274−278.

(14) (a) Jones II, L.; Schumm, J. S.; Tour, J. M. *J. Org. Chem.* **1997**, *62*, 1388−1410. (b) Tour, J. M.; Jones II, L.; Pearson, D. L.; Lamba, J. S.; Burgin, T.; Whitesides, G. M.; Allara, D. L.; Parikh, A. N.; Atre, S. *J. Am. Chem. Soc.* **1995**, *117*, 9529. (c) Pearson, D. L.; Tour, J. M. *J. Org. Chem.* **1997**, *62*, 1376−1387.

(15) Dhirani, A.-A.; Zehner, R. W.; Hsung, R. P.; Guyot-Sionnest, P.; Sita, L. R. *J. Am. Chem. Soc.* **1996**, *118*, 3319−3320.

(16) The Au films on mica substrates consisted of tabular grains with large Au{111} terraces which were ideal for STM studies. The poor end-to-end flatness of the mica substrate precluded their use for reflection IR. In contrast, the Au/Cr/SiO_2/Si films were extremely fine grained with small, poorly discernible Au{111} terraces which rendered them unsuitable for STM. The fine grain Au film and the excellent flatness of the Si substrates made these samples ideally suited for IRS.

(17) Nuzzo, R. G.; Fusco, F. A.; Allara, D. L. *J. Am. Chem. Soc.* **1987**, *109*, 2358−2367. Troughton, E. B. et al. *Langmuir* **1988**, *4*, 365−385.

(18) Millipore Purification Systems, Bedford, MA.

Solutions of **1a** and *n*-dodecanethiol $CH_3(CH_2)_{11}SH$ were prepared at 0.3−3.0 mM total thiol concentration. At these concentrations, both compounds are readily soluble in tetrahydrofuran (THF). The substrates were immersed in the solutions overnight at room temperature, after which the samples were withdrawn, rinsed in hexane (HPLC grade), acetone (HPLC grade), and ethanol (USP grade), and stored under inert atmosphere until immediately before analysis. Mica-supported samples were analyzed using STM. The companion samples were then characterized by ellipsometry, contact angle, and IRS to verify the thickness, quality, and composition of the assembled films.

Molecular films of two types were formed: (1) films deposited from a solution containing both thiols, **1b** and dodecanethiol (co-assembly); and (2) films deposited from a solution containing the alkanethiol followed by immersion in a solution containing **1b**, **2b**, or **3b** (insertion). Each solution was prepared immediately before use under a N_2 atmosphere. Teflon jars were cleaned before use in an ultrasound bath of acetone, hexane, and distilled THF. The thiol solutions for coassembled deposition were 0.3 mM in total adsorbate concentration in freshly distilled THF with an addition of excess NH_4OH to generate **1a** from **1b** in situ. After overnight solution exposure *(ca.* 18 h), the substrates were removed and triply washed in THF, acetone, and ethanol. Preparation of the mixed monolayers by insertion began with the formation of a standard dodecanethiol self-assembled film (prepared from 1 mM dodecanethiol in ethanol, overnight adsorption), followed by hexane, acetone, and ethanol washes. The films were characterized by infrared spectroscopy and ellipsometry and then placed into a 0.3 mM solution of the protected insertion molecule **1b** (or **2b** or **3b**) with addition of NH_4OH to generate **1a** from **1b** (or **2a** from **2b** or **3a** from **3b**) in situ. The samples were kept in these solutions for either 0.5 or 1 h. Samples were subsequently triply washed in THF, acetone, and ethanol. STM samples were stored under inert atmosphere until immediately before STM analysis. Companion samples prepared on silicon substrates were stored under Ar.

II.C. Infrared Spectroscopy. Infrared external reflection spectra (IRS) were collected using a N_2 (CO_2^- and H_2O^- free)-purged, custom-modified Fourier transform infrared spectrometer as described in detail elsewhere.[19] The spectral intensities are reported as reflectivities in absorption units, $-\log(R/R_0)$, where R_0 is the reflectivity of a reference sample prepared by freshly cleaning an evaporated gold substrate using a UV-ozone exposure.[20,21] For quantitative analysis of the film fraction of **1**, the 1500 cm^{-1} aromatic ring C−C stretching mode was used as the analytical peak, and the tilt of **1** in the mixed monolayers was assumed to be at the same angle as in a full monolayer of **1**.[14b] Similarly, for quantitative analysis of the film fraction of **2**, the 1350 cm^{-1} nitro symmetric stretch mode was used as the analytical peak, and the tilt of **2** in the mixed monolayers was assumed to be at the same angle as in a full monolayer of **2**.

II.D. Ellipsometry. Single wavelength ellipsometry (SWE) measurements were recorded at 632.8 nm (He−Ne laser) and used to determine film thickness as described elsewhere.[22] A value of 1.50 + 0i was assumed for the complex optical constant of the dodecanethiolate and mixed films and 1.55 + 0i assumed for the pure **1** monolayers. The spot-to-spot standard deviation on each sample was under 1 Å. The sample-to-sample variations were within ±1 Å, and averaging over multiple experiments gave standard deviations of ∼0.5 Å.

II.E. Scanning Tunneling Microscopy. The STM images were recorded using two different beetle-style scanning tunneling microscopes.[23] Both microscopes are housed in chambers that were purged with dry N_2 or Ar gas to minimize air exposure and to eliminate capillary condensation. All the samples studied were sufficiently conductive that we were able to use DC tunneling current to control the tip−sample separation. All images were recorded at large tunneling gap impedances, 10^{11} Ω or higher, to reduce perturbations to the alkanethiolate monolayers caused by imaging. Such high impedance measurements have recently been shown to open the possibility of imaging the molecular lattices of the shorter chain alkanethiolate monolayers.[5,6,9] Controlled geometry Pt/Ir STM tips were used as the scanning probes.[24] All images were recorded in constant tunneling current mode. STM piezoelectric scanner calibrations were performed by recording atomic resolution images of surfaces of known crystallography. One of the microscopes is a microwave frequency alternating current STM (ACSTM), the design and operation of which have been previously described.[10,25]

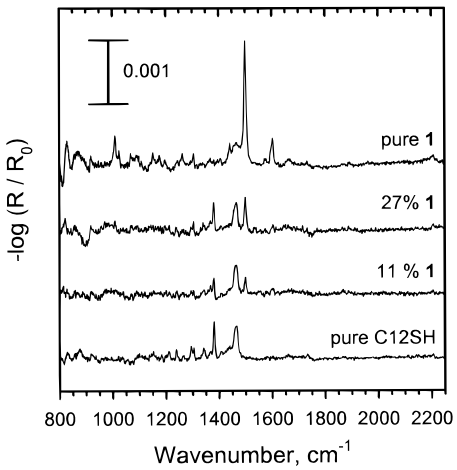

Figure 1. Low-frequency IRS spectra of co-assembled **1**/dodecanethiolate films. The 1500 cm^{-1} peak, an in-plane aromatic ring C−C stretching mode, is used to determine the relative amount of 1 in the film.

III. Characterization of the Average Film Structure

The average (macroscopic) structures of the mixed monolayers were characterized using SWE and IRS. The former provided insight into the quality of the films, in particular, cycles of thickness measurements coupled with multiple washings in THF and acetone provided assurances that the films were indeed monolayers of chemisorbed thiolates. Using IRS we deduced the percentages of **1**, **2**, or **3** in the monolayers and analyzed the alkyl C−H vibrations to determine the conformation of the dodecyl chains in the mixed monolayers.

To accomplish our goal of focusing on obtaining isolated oligomers surrounded by alkanethiol, most measurements were conducted on monolayers containing 25% or less oligomer (as compared to full monolayers of oligomers[15]). Measurements on full monolayers of oligomer were also conducted, however, and are included to provide reference points for the general trends taken from the data. Since measurements from coassembled and insertion monolayers show very different structures, the data are presented separately.

III.A. Coassembled Films. Figure 1 shows plots of the low-frequency infrared spectra taken from several coassemblies of **1a** and dodecanethiol. The 1500 cm^{-1} aromatic ring C−C stretching mode, because of its strong absorbance and isolation in the spectrum, was used as an analytical peak to quantify the fraction of **1** in the monolayers.[14b] Using this mode, a plot of SAM composition vs solution composition was constructed, shown in Figure 2. From these data, we infer that binding the dodecanethiol to the Au{111} surface is highly favored over binding **1a** to the surface. This contrasts with differential binding trends found for ω-functionalized alkanethiols by

(19) Parikh, A. N.; Allara, D. L. *J. Chem. Phys.* **1992**, *96*, 927−945.
(20) Vig, J. R. *J. Vac. Sci. Technol. A* **1985**, *3*, 1027−1032.
(21) UV-Clean, Model UV-C 100, Abtech, Yardley, PA.
(22) Laibinis, P. E.; Whitesides, G. M.; Allara, D. L.; Tao, Y.-T.; Parikh, A. N.; Nuzzo, R. G. *J. Am. Chem. Soc.* **1991**, *113*, 7152−7167.
(23) Besocke, K. *Surf. Sci.* **1987**, *181*, 145−153. Stranick, S. J.; Weiss, P. S. *Rev. Sci. Instrum.* **1994**, *65*, 918−921.
(24) Materials Analytical Services, Raleigh, NC.
(25) Stranick, S. J.; Weiss, P. S. *Rev. Sci. Instrum.* **1993**, *64*, 1232−1235. Stranick, S. J.; Weiss, P. S. *Rev. Sci. Instrum.* **1994**, *65*, 918−920. Bumm, L. A.; Weiss, P. S. *Rev. Sci. Instrum.* **1995**, *66*, 4140−4144.

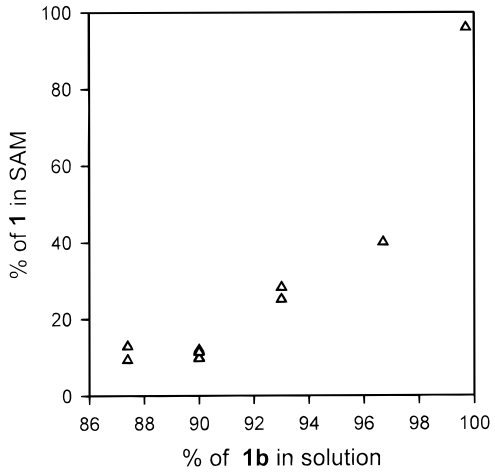

Figure 2. Plot of surface composition of **1** vs solution composition of **1a** for mixtures with dodecanethiol. Results from 10 separate depositions are shown.

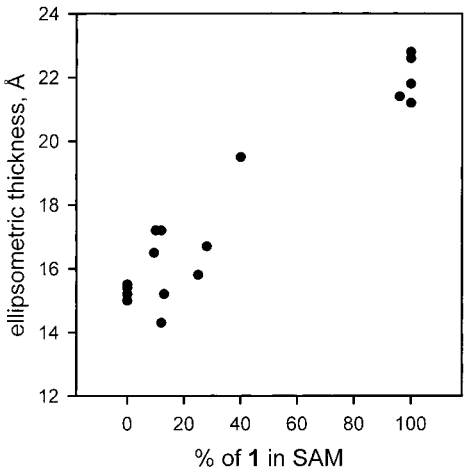

Figure 3. Experimental ellipsometric thickness (Å) vs percentage of **1** in a coassembled monolayer. Approximate values $n = 1.5$ and $k = 0.0$ were used for the ellipsometry calculations. Hard-sphere models of dodecanethiolate and **1** yield full extended lengths of ~15 Å and ~22 Å, respectively.

Whitesides and co-workers.[26] In mixed composition SAMs, ω-functionalized alkanethiols had higher surface concentrations relative to solution concentrations as their solubility decreased.[26] While **1a** is less soluble, it has a lower surface/solution composition than dodecanethiol. By measuring the concentration of **1** in the SAM we can use SWE to determine the thickness of the film. Figure 3 shows a plot of how the calculated thickness increases as the percentage of **1** increases in the film.

Figure 4 shows several IRS spectra of the C−H stretching region of the coassembled films of dodecanethiolate and **1**. As can be seen, the control film (containing no **1**) has spectra typical of those reported previously.[27] As the percentage of **1** in the film increases, several trends emerge. Figure 5 shows a plot of peak position for the methylene antisymmetric (d^-) and methylene symmetric (d^+) stretches of the coassembled films. Figure 6 shows a plot of the broadening of these modes when **1** is present in the film. Note that since both the dodecanethiolate and **1** have alkyl C−H bonds, the changes in the C−H stretching region cannot be accounted for by a simple linear combination of a spectrum of pure dodecanethiolate SAM and a spectrum of pure **1**. These perturbations in the C−H stretching region indicate that molecules of **1** cause the dodecanethiolate SAM to disorder to some extent. Note that a completely liquidlike state would have a d^- peak shifted even higher by

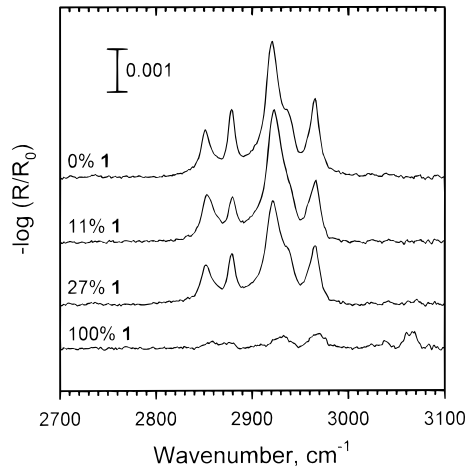

Figure 4. Infrared spectra of the C−H stretching region of different mixtures of coassembled **1**:dodecanethiolate monolayers.

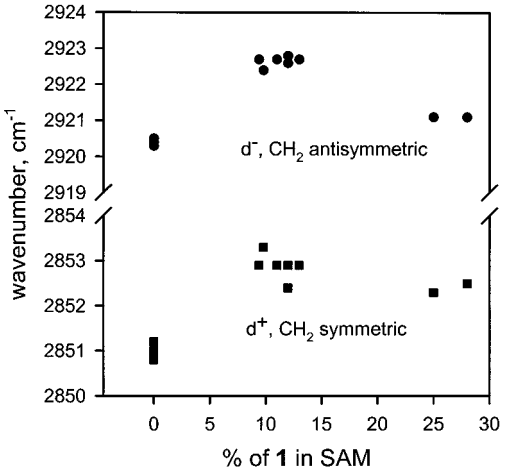

Figure 5. Peak positions of the antisymmetric (●) and symmetric (■) stretches of methylene groups in the coassembled **1**/dodecanethiolate monolayer.

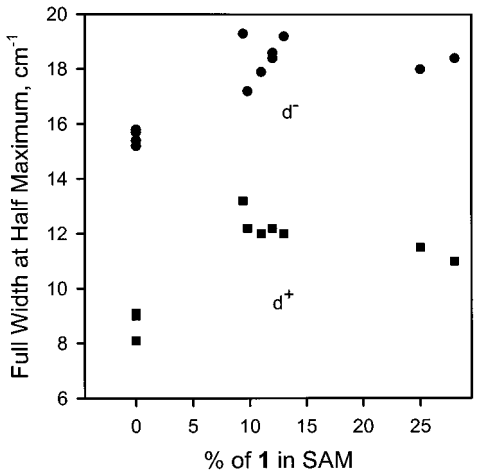

Figure 6. Peak widths at half-maximum of the antisymmetric (●) and symmetric (■) stretches of methylene groups in the coassembled **1**/dodecanethiolate monolayer.

(26) Bain, C. D.; Troughton, E. B.; Tao, Y.-T.; Evall, J., Whitesides, G. M.; Nuzzo, R. G. *J. Am. Chem. Soc.* **1989**, *111*, 321−335. Tam-Chang, S.-W.; Biebuyck, H. A.; Whitesides, G. M.; Jeon, N.; Nuzzo, R. G. *Langmuir* **1995**, *11*, 4371−4382.

(27) Porter, M. D.; Bright, T. B.; Allara, D. L.; Chidsey, C. E. D. *J. Am. Chem. Soc.* **1987**, *109*, 3559−3568.

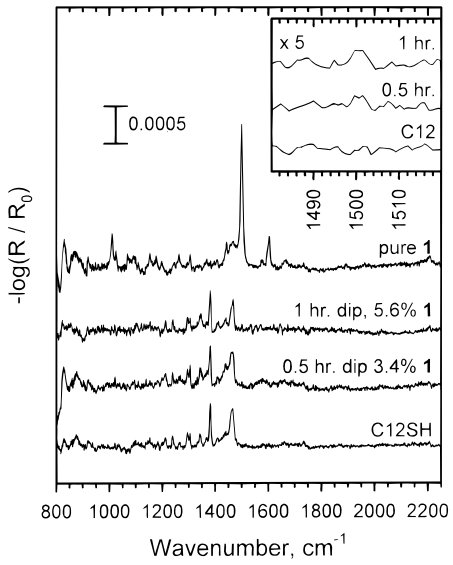

Figure 7. Low-frequency IRS spectra of dodecanethiolate monolayers immersed for different periods in a solution of **1a**. Pure dodecanethiolate and pure **1** monolayers are shown for comparison. The inset presents a magnification of the spectra near the 1500 cm^{-1} in-plane aromatic ring C−C stretching mode peak. This shows the detectability limit of 1 to be ∼2−3%.

∼5 cm^{-1}.[7b] Analysis of the low-frequency region reveals that the methylene scissoring (1465 cm^{-1}, broad) is still apparent as well as the methyl deformation (1380 cm^{-1}). The conservation of the general appearance of these peaks confirms that the overall structures of the alkyl chains are only partially disordered. Interestingly, the amount of disorder does not measurably increase as the percentage of **1** in the film increases.

III.B. Insertion Films. The low-frequency IR spectra of two insertion films and of two corresponding pure thiolate films are shown in Figure 7. In the insertion film spectra the signal from **1** is nearly obscured by the noise. However, the signal due to **1** was reproducible, as several repetitions of the spectra showed. Note that there is no discernible change in the C−H stretching region of the insertion monolayer as compared to that in the pure dodecanethiol monolayer. (The size of any perturbation is less than 0.5 cm^{-1} in peak position and 1.0 cm^{-1} peak width.) This lack of perturbation is very important with regard to interpreting the STM results.

While the maximum percentage of **1** in these films was ca. 6%, we have obtained similar results (no significant perturbation of CH_2 peak frequency or width) for film assemblies made by inserting up to 13% of **2a** into monolayers of dodecanethiolate on gold. In addition, independent results show that inserting **2** into *n*-alkanethiolate monolayers of 8, 10, 12, and 14 carbon chains results in **2** maintaining the same average tilt and twist as that of pure monolayers of **2**.[28]

IV. Single-Component Self-Assembled Monolayers

IV.A. Pure Alkanethiolates. Full alkanethiolate monolayers adopt a $(\sqrt{3} \times \sqrt{3})$R30° overlayer and related superstructures on the Au{111} substrate, with the chains assuming a ∼30° tilt to correct for the chain volume-sulfur spacing mismatch.[22,29] STM imaging of the alkanethiolate lattice can be accomplished, providing the tip−sample tunneling junction impedance is high enough that the tip does not strongly perturb the alkyl chains.[9,30,31] Due to experimental limitations in measuring tunneling currents less than ∼1 pA this condition can only be met for alkanethiol chain lengths which are sufficiently short (12 carbons or less in our study). The tunneling mechanism from the tip through these electrically insulating monolayers is still under study; theories include tunneling from the tip directly to the Au-bonded sulfur atoms (a through-space mechanism) or molecule-assisted tunneling (a through-bond mechanism).[31,32] In related work on coadsorbed *n*-alkanethiolates of different lengths, we observe that the alkyl chains do contribute to tunneling.[6] Sautet and co-workers have used an extended Hückel model to calculate the transmission current between a gold tip and a Au{111} surface with an alkanethiol molecule interposed.[33] For a dodecyl chain, the transmission current was calculated to be 1 pA at 50 mV, yielding a transresistance of 5×10^{10} Ω. This current (transresistance) decreases with increasing (decreasing) chain length.[6,33] This is consistent with experimental findings: Schonenberger et al. achieved molecular resolution of dodecanethiol at 3×10^{11} Ω tunneling resistance or greater;[30] Poirier and Tarlov found that a tunneling impedance of 10^9 Ω for "short-chain" monolayers and 10^{10} Ω for "long-chain" monolayers yielded the best tunneling conditions for imaging of the molecular lattice.[31] We set the tunneling impedance at or above 10^{11} Ω, which was sufficient in our system to resolve the alkanethiolate lattice.

Alkanethiol monolayers form flat, ordered terraces with single-Au atom high steps. The terraces are distinguished by domains of ordered lattices which frequently neighbor single-Au atom deep pits.[34] These pits contain alkanethiolates bound in the same close-packed conformation as on the terraces. The gold atoms in the terraces, therefore, are chemically isolated from the environment by the monolayer of close-packed alkane chains except at boundary areas such as step edges (either to another terrace or a pit) and alkanethiolate orientational domains (Figure 8). These boundary areas offer the greatest access to the underlying gold substrate and thus may offer the most favored sites for further chemisorption or Au electrochemistry. Electrochemical experiments have found that reduction or oxidation of a solvated species with the gold substrate is prevalent only when the solvated molecule is small enough to insert into the film and reach the gold substrate, at sites such as defects.[12,13,37] The electrochemistry of molecules unable to pass through the monolayer is greatly inhibited;[37] in this way the alkanethiolate monolayer forms an insulating barrier on the gold surface. These properties make the alkanethiolate monolayers ideal matrixes for inserting and isolating molecular wire candidates and for measuring their conductive properties.

(28) Cygan, M. T.; Dunbar, T. D.; Allara, D. L.; Tour, J. M.; Weiss, P. S. manuscript in preparation.

(29) Ulman, A.; Eilers, J. E.; Tillman, N. *Langmuir* **1989**, *5*, 1147−1152. Camillone, N.; Chidsey, C. E. D.; Liu, G.; Scoles, G. *J. Chem. Phys.* **1991**, *94*, 8493−8502. Fenter, P.; Eisenberger, P.; Liang, K. S. *Phys. Rev. Lett.* **1993**, *70*, 2447−2450.

(30) Schonenberger, C.; Jorritsma, J.; Sondag-Huethorst, J. A. M.; Fokkink, L. G. J. *J. Phys. Chem.* **1995**, *99*, 3259−3271.

(31) Poirier, G. E.; Tarlov, M. J. *Langmuir* **1994**, *10*, 2853−2856.

(32) Schonenberger, C.; Sondag-Huethorst, J. A. M.; Jorritsma, J.; Fokkink, G. L. *Langmuir* **1994**, *10*, 611−614.

(33) Salmeron, M.; Neubauer, G.; Folch, A.; Ogletree, D. F.; Sautet, P. *Langmuir* **1993**, *9*, 3600−3611.

(34) While these depressions have been attributed to a solution etching process,[30] observations of vapor-deposited films also find these same depressions.[12,35,36]

(35) McDermott, C. A.; McDermott, M. T.; Green, J.-B.; Porter, M. D. *J. Phys. Chem.* **1995**, *99*, 13257−13267.

(36) Poirier, G. E.; Pylant, E. D. *Science* **1996**, *272*, 1145−1148. Poirier, G. E. *Langmuir* **1997**, *13*, 2019−2026.

(37) Herr, B. R.; Mirkin, C. A. *J. Am. Chem. Soc.* **1994**, *116*, 1157−1158. Chailapakul, O.; Crooks, R. M. *Langmuir* **1995**, *11*, 1329−1340.

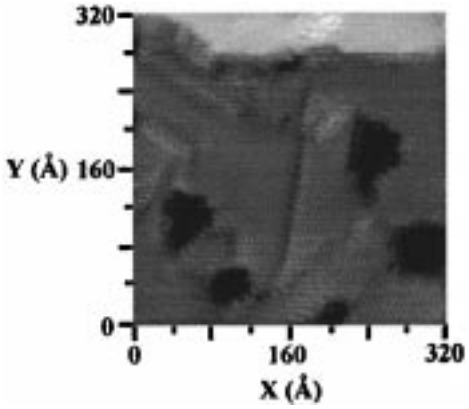

Figure 8. A constant-current STM topograph showing an area of an Au{111} surface covered by dodecanethiol (tip bias = +1.0 V, tunneling current = 10 pA). Film defects present include step edges, pits, and domain boundaries.

IV.B. Pure Oligomers. In contrast to the pure alkanethiolate monolayers, no order was observed for monolayers composed solely of **1**. Sita, Guyot-Sionnest, and co-workers were able to form ordered SAMs of a molecule closely related but lacking the ethyl functionalization of **1**.[15] The ethyl side group was added in our experiments to increase the solubility of **1a**. This strategy is required as the oligomer lengths increase to values which greatly reduce their solubilities. As our goal was to isolate individual oligomer molecules for electronic study, the ordering of pure monolayers of (molecules related to) **1** is purely incidental to our studies.

V. Conjugated Oligomers in Alkanethiolate Self-Assembled Monolayers

To study the electronic transport properties of single isolated molecules, these oligomers were incorporated into the alkanethiolate film as described in section II.B. Films formed by both deposition methods were imaged using the STM. Figures 9 and 10 are STM topographic images of films containing **1** deposited by simultaneous and successive depositions, respectively. These images are characteristic of a large number of analyses taken on films varying in **1**/alkanethiolate composition.

Coassembled films exhibit surface structures very different from those of pure alkanethiolate monolayers. Figure 9 typifies the surface topography of films resulting from simultaneous deposition. The structure of the underlying Au substrate is shown by the presence of step features of ~2.4 Å height separating wide (up to thousands of angstroms) terraces. However, no areas of the crystalline order characteristic of *n*-alkanethiolates were present, even at the lowest studied surface concentrations (11%) of **1**. We infer that the molecules of **1** disturb the ordering process of the alkanethiolates (which occurs through van der Waals interactions between the alkyl chains). This is supported by IR analyses (Figures 5 and 6) which show that coadsorbed films are more disordered as measured by the extent of gauche defects. The lack of order may be the result of molecules of **1** being present in many orientations, i.e., molecules of **1** could be attached to the Au substrate at many off-normal angles, forcing gauche defects in the dodecanethiolate film. Furthermore, the presence of **1** in any orientation would interrupt the long-range van der Waals interactions of the alkyl chains, leading to a decay of crystalline order. As the **1** molecules have a different structure and packing, alkanethiolates adjacent to **1** molecules will be less constrained to assume all trans conformations than those which are completely surrounded

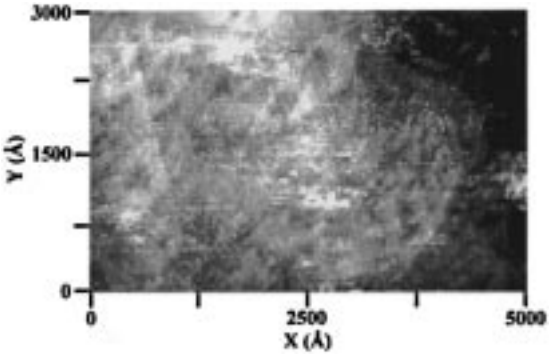

Figure 9. A constant current STM topograph of a co-assembled **1**/dodecanethiol monolayer. The area shown is 5000 Å × 3000 Å (tip bias = +1.0 V, tunneling current = 1 nA). The monolayer is ca. 25% **1**. The disordered terrace structure is due to the disruption of the alkanethiolate lattice caused by the presence of molecules of **1**.

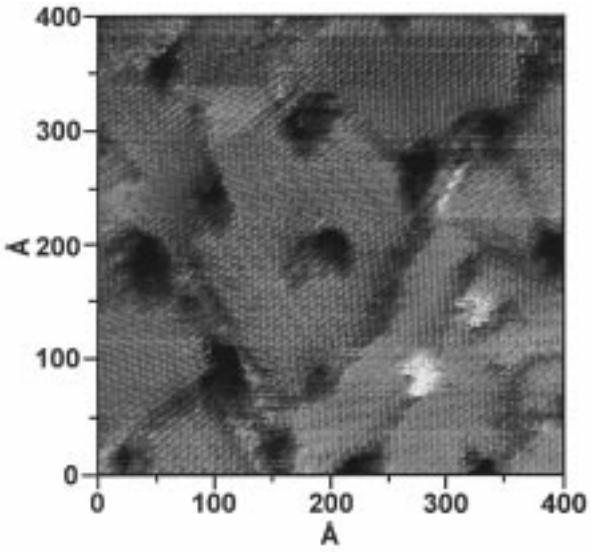

Figure 10. A constant current STM topograph of 400 Å × 400 Å area of a monolayer with inserted 1 (tip bias = +1.0 V, tunneling current = 10 pA). The overall monolayer is ca. 11% **1** by IRS. The molecules of **1** appear as peaks in topography (displayed as bright) and are indicated by arrows. They insert at structural domain boundaries in terraces of dodecanethiolate SAM.

by like molecules. There may be a critical film concentration of **1** which is low enough to permit the formation of a crystalline *n*-alkanethiolate lattice, but, if so, it is apparently below the lowest (11%) concentration studied here in coadsorption.

The insertion method results in monolayers quite distinct from those which are coassembled. Figure 11 is a schematic representation of molecules in an insertion monolayer. Figure 10 shows a representative constant-current STM image of a mixed **1**/dodecanethiolate monolayer formed by insertion. This molecular resolution image shows the crystalline order of the *n*-alkanethiolate monolayer. Pit defects and terrace domain boundaries are visible in the film as for pure alkanethiolate films. Protruding 4−6 Å from the film are features which we assign as **1**. These protrusions are absent in pure dodecanethiolate SAMs. Note that the features due to **1** appear broad because the protruding molecules of **1** image the tip structure as discussed previously.[10] Figure 12 shows the appearance of molecules of **1** scanned using a different probe tip. The appearance of **1** molecules is similar within a series of images scanned by the same tip, but the shape and size of the features vary with the structures of different probe tips. Note that due

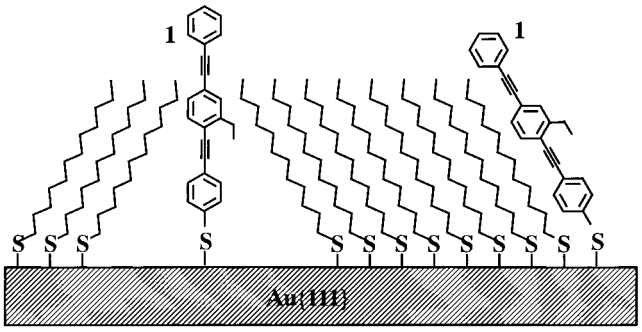

Figure 11. Schematic representation of the Au-bound molecular wire candidate molecule **1** in two possible orientations after insertion into a dodecanethiolate film. The tilted orientation shown on the right does not fit well within the crystalline alkanethiolate structure.

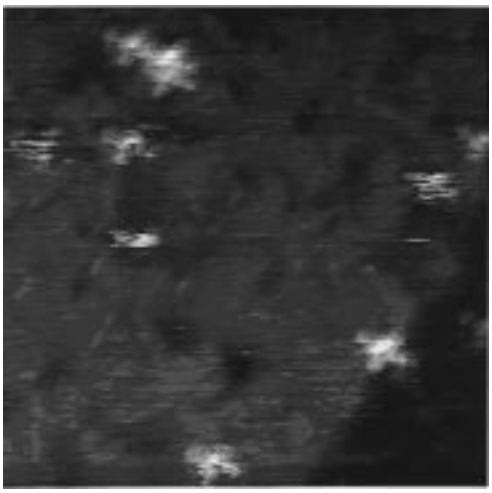

Figure 12. STM topograph of a 790 Å × 790 Å area of the same monolayer as that shown in Figure 10 under the same conditions but with a different STM probe tip.

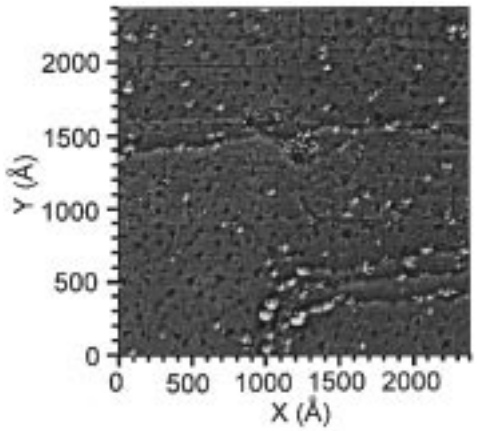

Figure 13. A larger area constant current STM topograph of a dodecanethiolate monolayer with inserted **1**. The area shown is 2400 Å × 2400 Å (tip bias = +1.0 V, tunneling current = 10 pA). The image has been high-pass filtered to bring out the structural detail on several Au terraces simultaneously.

to the particular shape of the STM probe tip, molecular resolution of the alkanethiolate lattice has been lost for this set of data. The molecules of **1** are located at both step edges and terrace domain boundaries (Figure 13), locations where the alkanethiolate film density is decreased. Thus, these locations offer increased access to the gold substrate, which in turn leads to lower barriers to chemisorption.

The **1**-derived features at the step edges are larger than those present at domain boundaries within terraces, indicating that step edge sites are able to accommodate a greater number of **1** molecules which can bond in close proximity to each other. The features due to **1** within domain boundaries on terraces are smaller and much more uniform in size and shape. The difference in feature size between these locations indicates that terrace domain boundaries are more selective; step edge sites permit adsorption of multimolecular "bundles", whereas terrace domain boundary sites allow only single (typically) or small numbers of molecules. Each of the single protruding features at domain boundaries in images such as Figure 13 cannot individually be assigned as single molecules. While the full-width-half-maximum of the protrusions appears to be 12 Å or greater, the imaging of the tip structure by the **1** molecules causes the imaged feature diameters to correspond to that of the tip shape rather than the diameter of the **1** molecules. We occasionally find a distorted feature which appears to be the convolution of two neighboring molecules of **1**. From these measurements, we believe that the overwhelming majority of identical protruding features at structural domain boundaries are due to single inserted molecules of **1**. As **1a** is not known to be aggregated in solutions, adsorption of aggregates would be unlikely. This is also consistent with the limited solution access through the film to the Au substrate at these sites.[12]

Molecules of **1** have not been observed to migrate within the film on time scales of hours. Figures 14a−d represent molecules of **1** in a dodecanethiolate SAM over a period of 4 h. Although thermal drifts shift the locations of the imaged area somewhat (i.e., the tip is imaging a slightly different section of the surface each image), the features due to **1** remain in the boundary defects at a constant distance from each other. This indicates some combination of strong chemisorptive binding and steric hindrance which retards the migration of the inserted molecules of **1** at these sites.

Corroborating results have been observed with similar systems using the insertion method. Molecules of **2** and **3** were inserted into monolayers of tetradecanethiolate, dodecanethiolate, decanethiolate, and octanethiolate under similar conditions to those used for **1**. Figure 15 shows a representative constant-current image of a dodecanethiolate monolayer with molecules of **2** inserted. As observed previously, the inserted molecules lie at defect sites in the film. The profile of the features due to **2** features are similar to those of the molecules of **1**. The features due to **2** protrude less from the dodecanethiolate film (ca. 2 Å compared to 6 Å) than did the features due to **1** under identical tunneling conditions and tips capable of dodecanethiolate lattice resolution. This difference is less than the difference of the molecular lengths of **1** and **2** (ca. 6 Å). We note that STM is *not expected* to give topographic features representative of molecular length.[6,33,38] Experiments also show that in topographic images, **2** protrudes from a tetradecanethiolate layer by at least 2 Å (Figure 16), whereas if it is normal to the substrate, it would be at least 1 Å physically *shorter* than the thickness of the (tilted) tetradecanethiolate layer. This indicates that there are significant electronic tunneling effects that result in images which do not match the physical topography.

Figure 17a is a representative image of an octanethiolate film with inserted **3** molecules. Pit defects and terrace domain boundaries are visible in the film. Protruding from the film are features which we assign to the molecules of **3**. Although

(38) Eigler, D. M.; Weiss, P. S.; Schweizer, E. K.; Lang, N. D. *Phys. Rev. Lett.* **1991**, *66*, 1189−1192. Weiss, P. S.; Eigler, D. M. *Phys. Rev. Lett.* **1993**, *71*, 3139−3142. Weiss, P. S. *Trends Anal. Chem.* **1994**, *13*, 61−67.

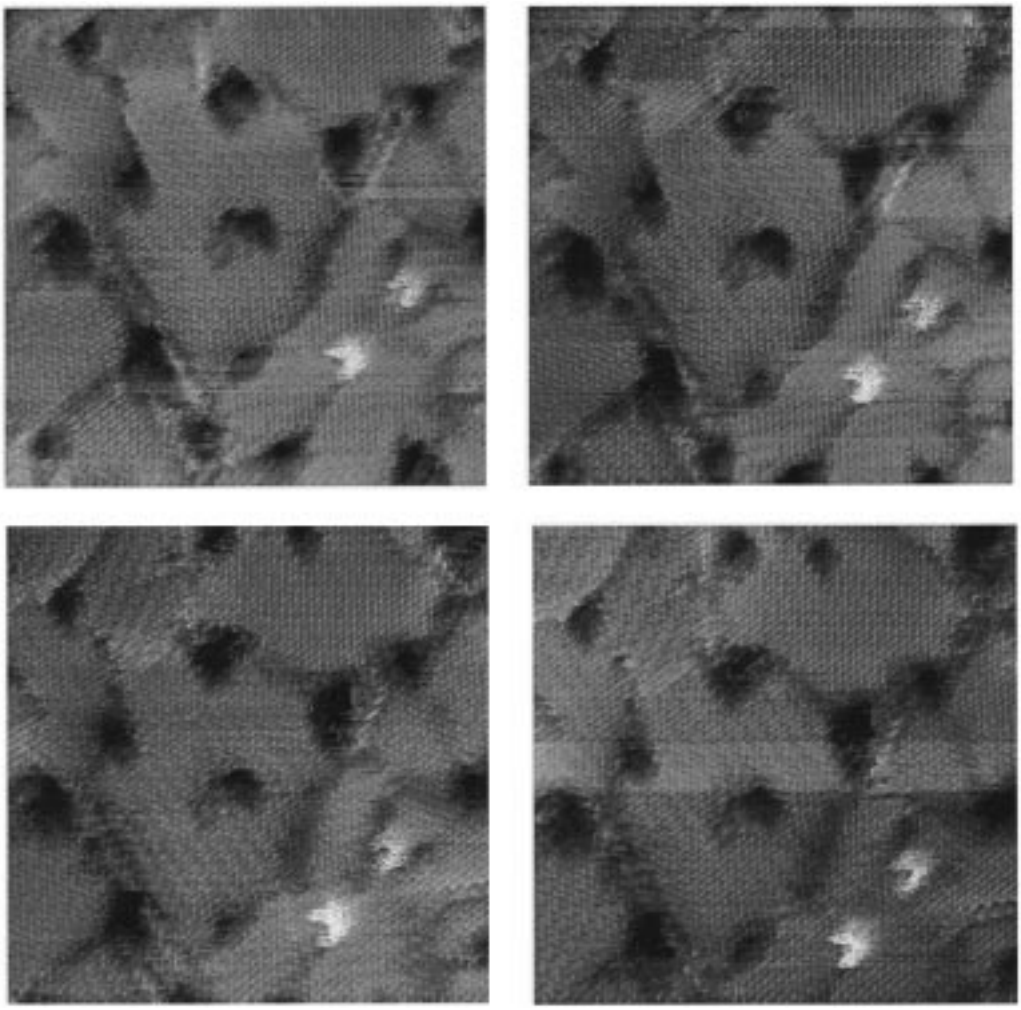

Figure 14. Topographs a−d are successive scans over an area of an insertion film. The features due to **1** remain at a constant distance from each other and do not migrate. The area imaged shifts slightly toward the bottom of the images due to thermal drift of the tip and sample. Scan initiation times: (a, top left) 0; (b, top right) 20; (c, bottom left) 40; and (d, bottom right) 60 min.

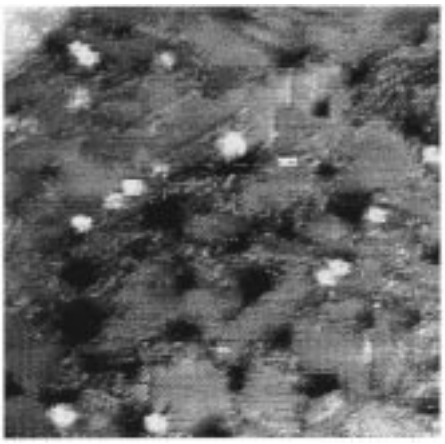

Figure 15. A constant current STM topograph of a dodecanethiolate film with inserted molecules of **2**. The film was formed by immersion of a nominally complete dodecanethiolate/Au film into a 0.3 mM solution of **2a** in THF for 14.5 h. The area shown is 400 Å × 400 Å (tip bias +1.0 V, tunneling current 5 pA).

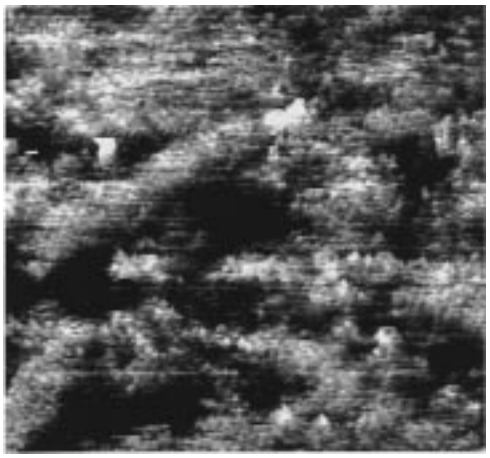

Figure 16. STM image of a 175 Å × 160 Å area of a tetradecanethiolate monolayer containing inserted molecules of **2**. Molecules of **2** appear at domain boundaries. The tunneling conditions were 1 V bias and 2 pA tunneling current.

the alkanethiolate lattice has not been fully resolved, rows representing the orientational domains of octanethiolates are visible. Although this image shows some streaking in the fast scan direction (horizontal), the inserted oligomers are resolvable. This is noteworthy due to the "extreme" length of the inserted **3** oligomer. With a molecular length of 41 Å, the molecule may protrude physically from the octanethiolate film as much as 33 Å.

Figure 17b is a three-dimensional rendering of Figure 17a which more clearly shows the oligomer features. Each oligomer appears in STM imaging as an 8−10 Å protrusion from the

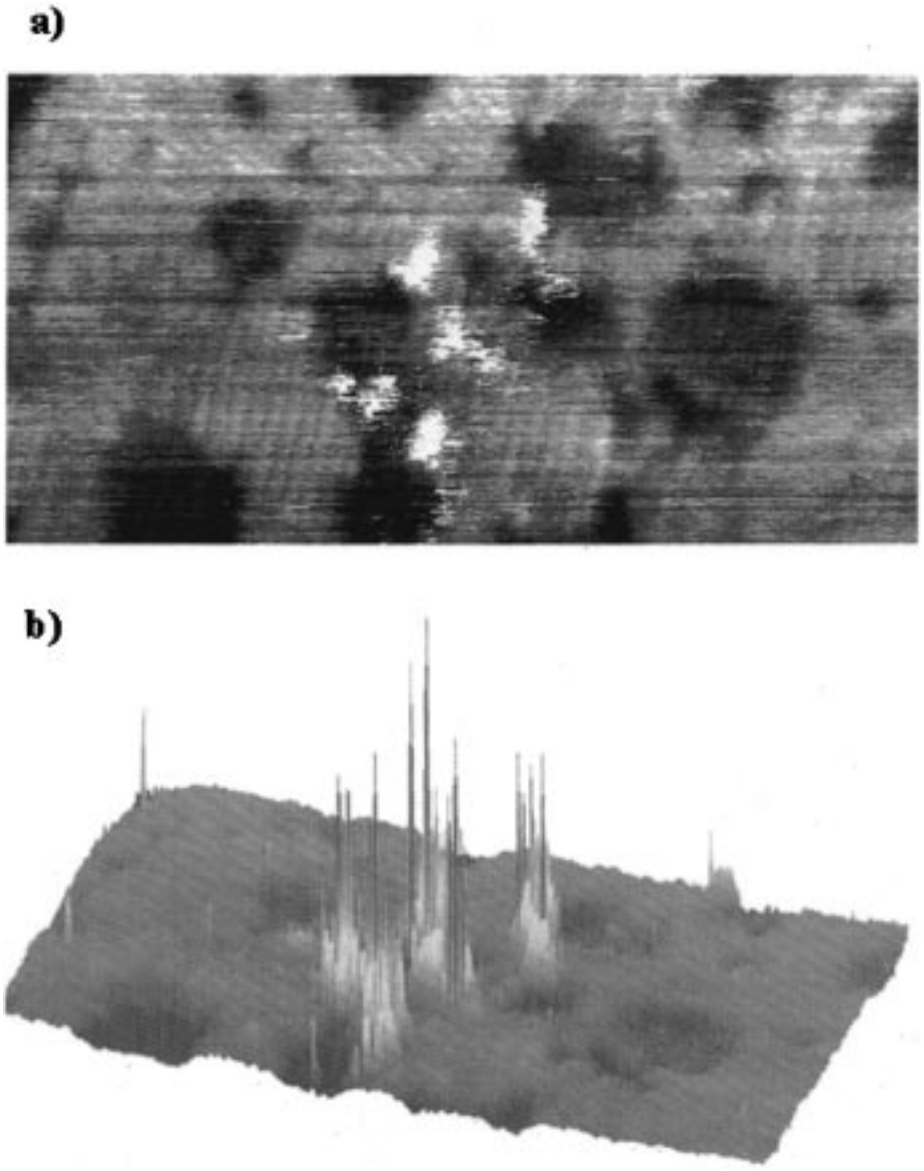

Figure 17. (a) STM image of a 200 Å × 300 Å area of an octanethiolate monolayer containing inserted molecules of **3**. Molecules of **3** are present at domain boundaries near pit defects. The tunneling conditions were 1 V bias and 3 pA tunneling current. (b) Three-dimensional STM image of a 200 Å × 300 Å area of an octanethiolate monolayer containing inserted molecules of **3**. Current spikes with topographic heights ranging from 20 Å to 40 Å are present at the features representing molecules of **3**. The tunneling conditions were 1 V bias and 3 pA tunneling current.

film. Extending from each protrusion are a number of spikes which extend as much as 40 Å from the octanethiolate film corresponding to the tip withdrawing this far during constant current imaging. These spikes have only been observed for alkanethiolate films with inserted **3** molecules and then only at the **3** oligomer features. The spikes are clearly distinguishable from noise as the spikes are always in the direction of increasing tip−sample separation. The spikes, which always accompany the oligomer features, represent jumps of increased current when the STM probe tip is placed near or perhaps in contact with an oligomer molecule.

For each oligomer/alkanethiolate film studied, the STM images show oligomer protrusion heights which increase with increasing oligomer length. The oligomer **2**, containing two phenyl rings, appears as 2−3 Å topographic protrusions from the film. The oligomer **1**, containing three phenyl rings, appears as 4−6 Å topographic protrusions from the film. The oligomer **3**, containing six phenyl rings, appears as 8−10 Å topographic protrusions from the film with even higher spikes. A more complete treatment of STM imaging of the oligomer will follow in a future paper.[28]

VI. Electron Transport Properties of Insertion Films

Previous studies of electron transport through conjugated aromatic thiols have been undertaken through field emission,[39] break junction,[40] network connection,[41] and microcontact[42] experiments as well as theoretical computation.[43] We have used

(39) Purcell, S. T.; Garcia, N.; Binh, V. T.; Jones II, L.; Tour, J. M. *J. Am. Chem. Soc.* **1994**, *116*, 11985−11989.

(40) Reed, M. A.; Zhou, C.; Muller, C. J.; Burgin, T. P.; Tour, J. M. *Science* **1997**, *278*, 252−254.

(41) Andres, R. P.; Bein, T.; Dorogi, M.; Feng, S.; Henderson, J. I.; Kubiak, C. P.; Mahoney, W., Osifchin, R. G.; Reifenberger, R. *Science* **1996**, *272*, 1323−1325.

(42) Zhou, C.; Deshpande, M. R.; Reed, M. A.; Jones, L., II.; Tour, J. M. *Appl. Phys. Lett.* **1997**, *71*, 611−613.

(43) Samanta, M. P.; Tian, W.; Datta, S.; Henderson, J. I.; Kubiak, C. P. *Phys. Rev. B* **1996**, *53*, R7626−R7629. Mujica, V.; Kemp, M.; Roitberg, A.; Ratner, M. *J. Chem. Phys.* **1996**, *18*, 7296−7305. Mujica, V.; Kemp, M.; Ratner, M. A. *J. Chem. Phys.* **1994**, *8*, 6856−6864.

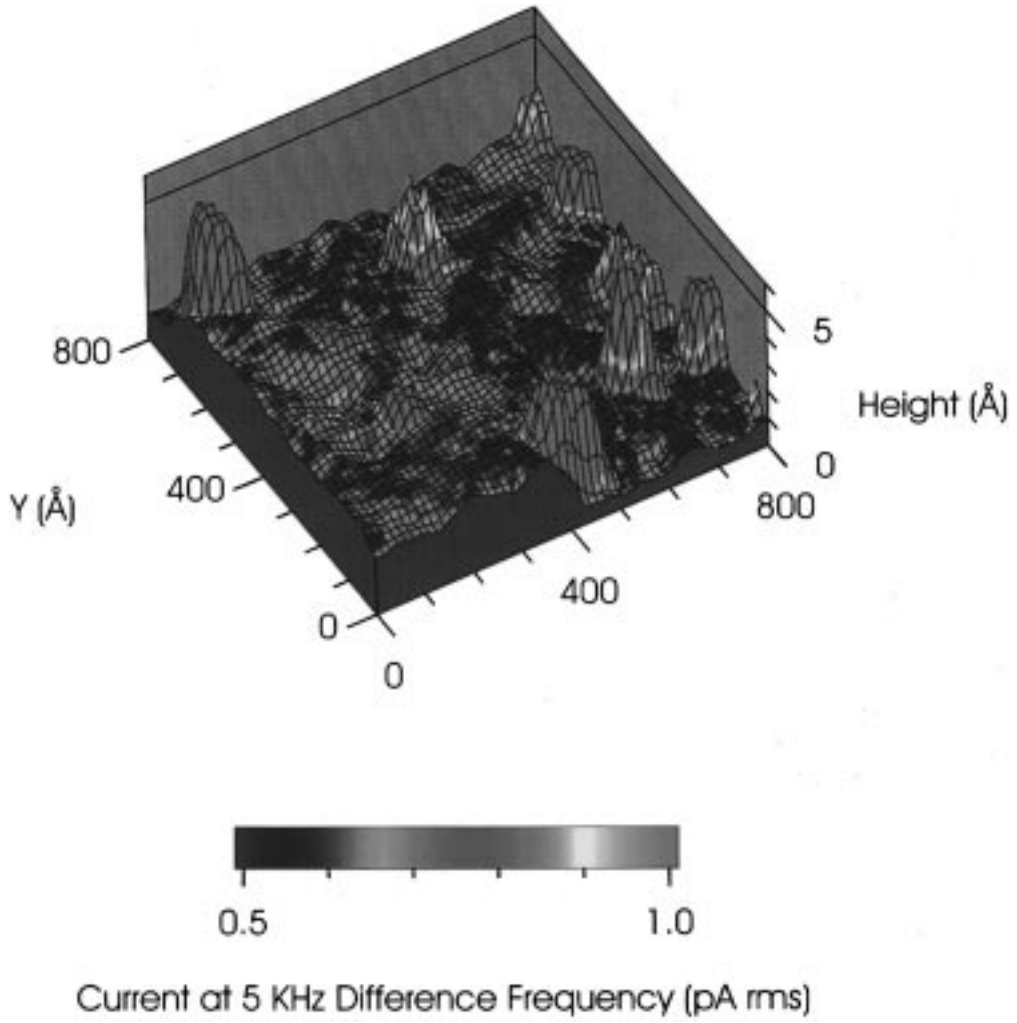

Figure 18. A composite ACSTM image of an 800 Å × 800 Å of a dodecanethiolate monolayer with inserted **1**. The surface is derived from the constant-current topograph, and the color is derived from the microwave difference signal (dc tip bias, 1.0 V; dc tunneling current, 10 pA; microwave frequencies, 5.000 000 00 and 5.000 005 00 GHz applied to the ACSTM tip transmission line at about 1 mW each; detection at 5 kHz).

a microwave frequency alternating current STM (ACSTM) to undertake two conductivity measurements of the insertion **1**/dodecanethiolate film: high-frequency electron transmission through the ACSTM tip-**1**−Au substrate junction and the apparent tunneling barrier height (ATBH) of the junction. In the first method, two microwave frequency components (separated by 5 kHz) are added to the dc bias between tip and sample. The component of the tunneling current at the difference frequency is extracted with a phase-sensitive detector and recorded as a separate image channel simultaneous to the conventional dc STM topographic image.[10] Figure 18 is a three-dimensional representation of the constant current topography of a typical area overlaid with a color scale corresponding to the intensity of the difference frequency signal. While the dodecanethiolate lattice is at a median height and intensity, the protrusions due to **1** exhibit marked increases or decreases in intensity. In the majority of these measurements, inserted molecules of **1** exhibited a difference signal of greater intensity than the dodecanethiolate lattice, indicating that these are areas of greater conductance than the alkanethiolate lattice. Figure 19 features a decanethiolate monolayer containing inserted molecules of **2**. The representation is the same as for Figure 18. The molecules of **2** shown in Figure 19 also exhibit increased difference frequency signal intensity. We attribute this increase to a conductive property of the phenylene ethynylene backbones of the inserted molecules.

For molecules of **1** and **2**, this can be understood in terms of the highly conjugated molecular structure, relative to the alkanethiolate, which facilitates electron transport through a delocalized p orbital structure. We note that these measurements were made with a dc bias of 1 V and that we have not yet made spectroscopic measurements to determine the existence or absence of a band gap for these oligomers.

In the second set of measurements, the ATBH is probed by modulating the tip−sample separation perpendicular to the surface (*z*) and recording the derivative of the tunneling current (i) with respect to this separation (*di*/*dz*).[44] The ATBH is found to be at least twice as high when the junction contains a **1** molecule than when the junction contains only dodecanethiolate molecules. Since ATBH measurements involve physical factors which we are not able to quantify (such as mechanical distortions of the tip and film),[44,45] we do not attempt to identify the exact nature of the ATBH increase. However, in qualitative terms, the greater degree to which the tunneling current changes (over a certain *z* distance) through a junction containing **1** than a junction containing dodecanethiolate may result from (1) a greater number of accessible surface states (over the *z* range)

(44) See, for example: Chen, C. J. *Introduction to Scanning Tunneling Microscopy*; Oxford University Press: New York, 1993.

(45) Olesen, L.; Brandbyge, M.; Sørensen, M. R.; Jacobsen, K. W.; Lægsgaard, E.; Stensgaard, I.; Besenbacher, F. *Phys. Rev. Lett.* **1996**, *76*, 1485−1488. Pecina, O.; Schmickler, W.; Chan, K. Y.; Henderson, D. J. *J. Electroanal. Chem.* **1995**, *396*, 303−307.

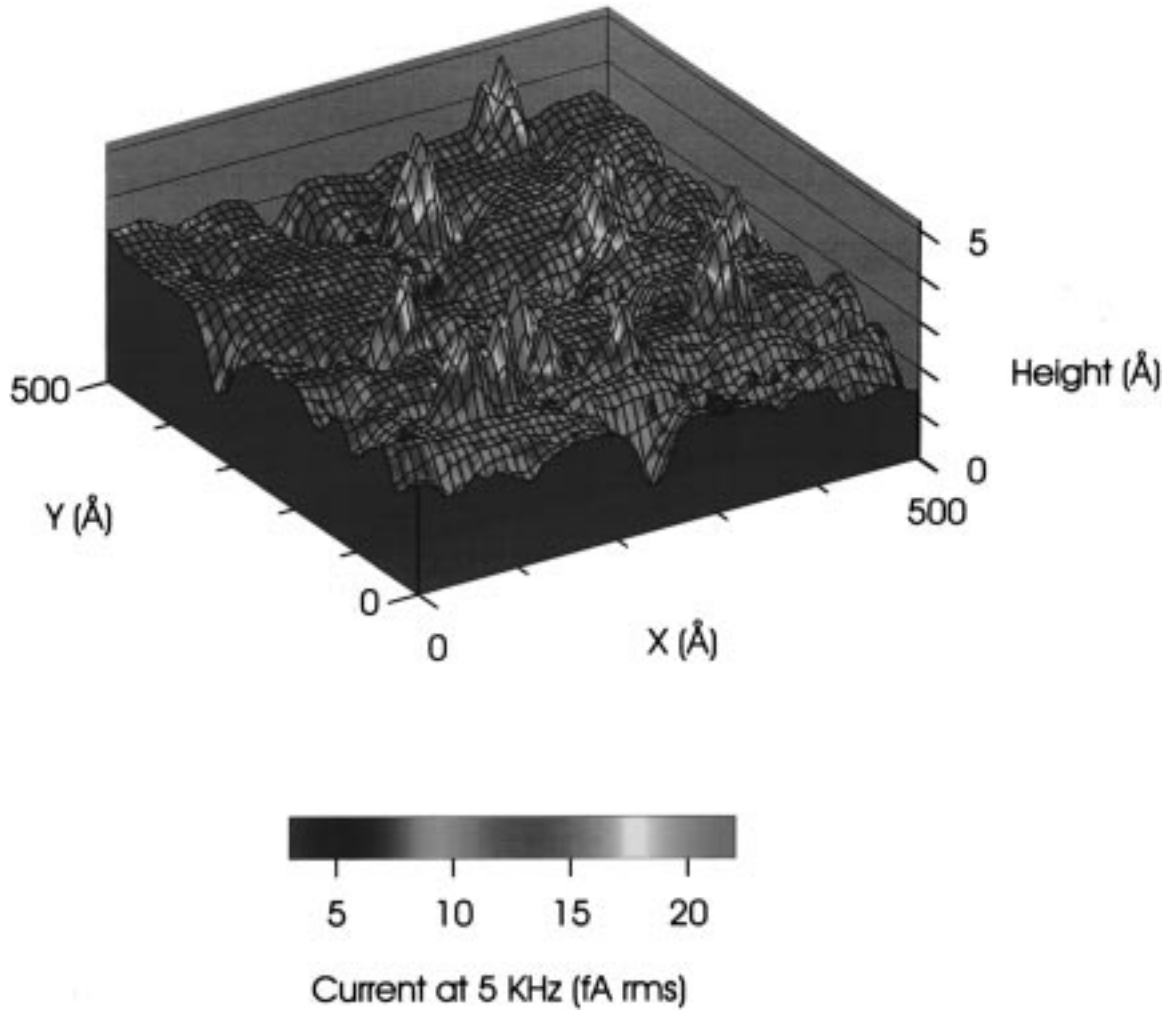

Figure 19. A composite ACSTM image of an 500 Å × 500 Å of a dodecanethiolate monolayer with inserted **2**. The surface is derived from the constant-current topograph, and the color is derived from the microwave difference signal (dc tip bias, 1.0 V; dc tunneling current, 10 pA; microwave frequencies, 5.000 000 00 and 5.000 005 00 GHz applied to the ACSTM tip transmission line at about 1 mW each; detection at 5 kHz).

due to **1** or (2) a **1**-induced extension of the bulk Au electron density (i.e., the exponential decrease in the Au wave functions extending out from the bulk Au is delayed or otherwise modulated by the presence of **1**), causing the current vs voltage slope to be steeper than that of the corresponding behavior of the tip-dodecanethiol-Au junction.

In both the ATBH and microwave difference frequency experiments, we find that the nature of the tip-**1** tunneling junction is fundamentally different from that of the tip-dodecanethiolate/Au junction. We infer from this that **1** is more active in modulating electron transfer from the tip to the Au substrate than the dodecanethiolate SAM. Further experimentation is in progress with similar molecules (such as **2**) to understand further the nature of this modulation.[28]

VII. Conclusions and Prospects

In summary, we have shown the ability to insert molecules of interest into specific sites in an alkanethiolate film matrix while preserving the surrounding structure. We have also contrasted the surface structures resulting from different deposition methods and from these structures elucidated information about the assembly process between two dissimilar self-assembling molecules. In coassembled films, we find structural disorder, which may indicate a number of possible binding orientations for the molecules of **1** and greater chain disorder in the dodecanethiolates. When **1** is inserted into an already assembled alkanethiolate film, it binds preferentially at step edges and structural domain boundaries on ordered Au{111} terraces and is not observed to migrate under observation periods of hours. Such insertion films show no observable loss in the alkanethiolate lattice ordering and isolate the conjugated oligomers as single molecules and as bundles for further study of their electronic characteristics.

While valuable here for matrix isolation studies, having the molecules placed in a variety of different defect sites may be undesirable for applications in molecular electronics. In our continuing research in this area, we seek to control the defect type and density in SAMs which can then be used to insert molecules selectively.[6] Ultimately, it will likely be necessary to place the molecules either in regular positions or in predetermined positions determined by patterning. Such strategies may well be able to employ any of a number of novel means proposed for placing or removing organic molecules from surfaces.[46]

Using an ACSTM, we can show contrast between the high frequency conductivity of the conjugated oligomers and the surrounding alkanethiolate matrix. We find that tunneling

(46) Sun, L.; Crooks, R. M. *Langmuir* **1993**, *9*, 1951−1954. Kumar, A.; Abbott, N. L.; Kim, E.; Biebuyck, H. A.; Whitesides, G. M. *Acc. Chem. Res* **1995**, *28*, 219−226. Seshadri, K.; Froyd, K.; Parikh, A. N.; Allara, D. L.; Lercel, M. J.; Craighead, H. G. *J. Phys. Chem.* **1996**, *100*, 15900−15909. Tarlov, M. J.; Burgess, D. R. F., Jr.; Gillen, G. *J. Am. Chem. Soc.* **1993**, *115*, 5305−5307. Xu, S.; Liu, G.-Y. *Langmuir* **1997**, *13*, 127−129.

junctions composed of a probe tip, a highly conjugated molecule, and a gold substrate exhibit greater conductivity than junctions composed of a probe tip, an alkanethiolate, and a gold substrate. This offers the possibility of creating stable nanometer-scale structures within surface films through self-assembly methods as well as future directions for design of molecule-specific devices such as chemical sensors and nanometer-scale electronic components.

Acknowledgment. The support of the National Science Foundation Chemistry, Graduate Research Traineeship, Presidential Young Investigator Programs, the Office of Naval Research (the above for M.T.C., J.J.A., L.A.B., N.F.S., and P.S.W.), the National Science Foundation Research Experiences for Undergraduates Program (for N.F.S. and P.S.W.), the Alfred P. Sloan Foundation (for P.S.W.), and the Defense Advanced Research Projects Agency (for T.D.D., T.P.B., L.J., D.L.A., and J.M.T.) are gratefully acknowledged.

Supporting Information Available: Spectral data for compounds 2b and 3b (1 page). See any current masthead page for ordering and Web access instructions.

JA973448H